DOI: 10.13009/EUCASS2019-908

Safety Motion Planning for Spacecraft Autonomous Proximity Maneuver

Xueping Wang , Xin Ning*,Xiaona Liu**
**127 West Youyi Road, Northwestern Polytechnical University, Xi'an Shaanxi, 710072, P.R.China.*
wxp262816@mail.nwpu.edu.cn
ningxin@nwpu.edu.cn
lxnove@mail.nwpu.edu.cn

Abstract

This paper proposes a novel method to solve autonomous proximity maneuver to an uncooperative target in the final phase of RVD (Rendezvous and Docking) mission. Close-range relative motion between space vehicles exists attitude-orbit coupling, especially for uncooperative target. The primary reason of coupling is conversions of multiple coordinate systems. Based on this, a uniform attitude-orbit-coupling dynamic model in LVLH coordinate is established. Then a PD-like controller is utilized to achieve the attitude tracking of the target. In addition, the servicer would access to the target considering the geometry of the target and the approaching corridor. To guarantee the safety of trajectory under the interference of coupling, a special Artificial Potential Function (APF) is developed. In geometric interpretation, the target are enveloped in combination of ellipsoid and cone as repulsive potential functions. These geometries of the target represent the main body, components and the approach corridor respectively. Afterwards, based on APF, a safe path planning scheme which includes coupling term is designed. The servicer would reach the docking port with attitude synchronization, and the trajectory would propagate in safety workspace. Simulations of uncooperative spacecraft proximity maneuver is performed to illustrate the effectiveness of the proposed method.

1. Introduction

With the continuous increase amount of spacecraft launched into orbits, high-cost astrovehicles are exposed to more challenges such as components damage, fuel exhaustion, orbit decay, etc. Once these crises appear, spacecraft would become space debris or fall into the atmoshpere inevitably. It can results in huge economic losses and serious space security issues. For these reasons, autonomous on-orbit service technology for uncooperative object has great application value and prospects in space nowadays. Previous researches and projects mainly concerned with normal and cooperative spacecraft, such as AFDL's Experiment Satellite System(XSS)[1], Demonstration of Autonomous Rendezvous Technology (DART) project[2] performed by NASA, DARPA's Orbital Express (OE) project[3], Phoenix project[4] and Synchronized Position Hold Engage Reorient Experimental Satellite (SPHERES) test-bed[5]. JAXA's Engineering Test Satellite[6] (ETS-VII), etc. However, Few studies have comprehensively considered both attitude-orbit coupling and safe motion planning during the approach process for uncooperative spacecraft.

In the relative motion of two spacecraft in close range, the relative attitude motion is independent while the relative orbital motion is coupled with the attitude. It will be analyzed in detail below. At present, the investigations of spacecraft attitude tracking have yielded substantial achievements. Lizarralde F, et al[7] presented a method to exploit the inherent passivity of the system, which replaces the the angular velocity feedback by a nonlinear filter of the quaternion. Jin E, et al[8] explored two controllers based on unit quaternion attitude parameterization to guarantee finite time reachability of given desired attitude motion, where model uncertainties and external disturbances are considered. An-Min Zou, et al[9] proposed a distributed output feedback attitude coordination control scheme to solve attitude coordination control problem for spacecraft formation flying. Yaguang Yang[10] proposed an efficient algorithm for the periodic discrete-time Riccati equation arising from a linear periodic time-varying system. It can be adopted in spacecraft attitude control using magnetic torques.

Several path planning methodologies for sapcecraft proximity maneuver have been investigated over the past decades, such as graph theory, optimal control, potential field method, parameter optimization method, way-points method, variational method, linear programming method, A* search method, random Optimization method, etc. Roger, et al[11] discussed the safety-limited trajectory planning of robots flying around the International Space Station through the use of artificial Laplace potential functions within a constrained volum. Liu Xinfu and Lu Ping[12][13] presents a

DOI: 10.13009/EUCASS2019-908

methodology to convert the initial nonconvex optimal control problems of autonomous rendezvous and proximity operations (RPO) into second-order cone programming problems. It has high reliability of finding the solution and requires no externally supplied initial guesses. Louis Breger, et al[14] proposed a method for online generation of safe, fuel-optimized rendezvous trajectories, and a convex formulation of the collision avoidance algorithm is introduced and shown to provide much faster solutions with only a small additional fuel expense.

The artificial potential function (APF) is a kind of typical analytic method which is first proposed by Khatib[15] and widely used in the path planning for the ground robots. Because of its intuitive mathematical form and less computation, it is suitable for path planning and obstacle avoidance in spacecraft's proximity maneuver procedure. Nicholas Martinson and Josue D. Munoz[16] addresses a new concept based on potential function for close proximity operations in space. Ender St.John–Olcayto, et al[17] detailed the development and evaluation of potential function guidance for path constrained proximity maneuvers of spacecraft at the International Space Station. Josue D. Munoz,et al[18] proposed an Adaptive Artificial Potential Function methodology for rapid path-planning of spacecraft autonomous proximity operations in subsequent study. This method permits attractive potential with time dependent weights which are defined by an adaptive update law. In this paper, an unique dynamic artifial potential function is design for the servicer-target system, and motion planning including attitude synchronization is addressed to solve the proximity maneuver problem.

The rest paper is organized as follows : Section 2 give the relative dynamic model and the factors of coupling is analyzed. In section 3, attractive and repulsive potential functions are formulated respectively and a whole artificial potential function is given. Motion planning scheme of proximity maneuver is detailed in section 4, and in section 5, numerical simulation are carried out to comfirm the effectiveness. Finally, conclusions are summarized in section 6.

2. Problem Statement and Relative Motion Model

The problems concerned in this paper is to driving a service spacecraft safely and autonomously approach an uncooperative target in space. As the target body rotates, the orientation of docking axis changes with time in sapce, and the safety corridor defined by docking axis is not constant. In addition, tumbling target components(e.g. solar panels, satellite antenna and other compartment of sation) would interfere with the safety of approach path in extra-close range.These pose great challenges to the servicer's coordinated planning of attitude and orbit. It assumes that the target is in an elliptical orbit and various perturbation factors are ignored. This assumption is reasonable because of short-time approaching process.

2.1 Coordinate Frames

Coordinate frames system invovled in this paper is as fellows :

(1) Earth-centre inertial frame (ECI) :$\mathcal{F}_I = \{O_I, X_I, Y_I, Z_I\}$,wherein the origin is at the centre of the Earth ; $O_I X_I$ axis points to vernal equinox ; $O_I Y_I$ axis is perpendicular to $O_I X_I$ axis and the $X_I Y_I$ plane coincides with the Earth's equatorial plane ; $O_I Z_I$ axis is perpendicular to the equatorial plane and points to the north pole.

(2) Loacl vertical Local horizontal frame (LVLH) : $\mathcal{F}_L = \{O_t, X_L, Y_L, Z_L\}$, wherein the origin is at the centroid of target ; $O_t X_L$ axis points from the center of the Earth to the target centroid ; $O_t X_L$ axis is along the direction of the orbit velocity; $O_t Z_L$ axis is perpendicular to the orbital plane ; $O_t Y_L$, $O_t X_L$ and $O_t Z_L$ satisfy the right-hand rule.

(3) Taget body coordinate frame : $\mathcal{F}_t = \{O_t, X_t, Y_t, Z_t\}$, wherein the origin is at the centroid of the target ; $O_t X_t$, $O_t Y_t$ and $O_t Z_t$ are aligned with principal body axes.

(4) Servicer body coordinate frame : $\mathcal{F}_s = \{O_s, X_s, Y_s, Z_s\}$, wherein the origin is at the centroid of the servicer ; $O_s X_s$, $O_s Y_s$ and $O_s Z_s$ are aligned with principal body axes.

2.2 Relative Attitude Dynamic

In past researches, serval mathematical tools were utilized to describe the attitude dynamic of spacecraft. In this paper, becasue of the advantages of nonsingularity, Qaternion is applied to construct relative attitude dynamic equation.

DOI: 10.13009/EUCASS2019-908

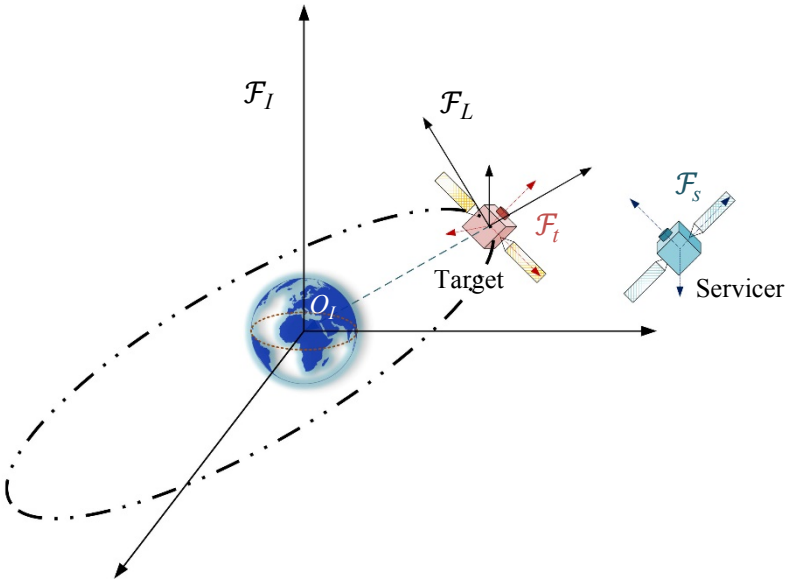

Figure 1: Coordinate Frames

As the assumption that perturbation factors aren't took in consideration, the attitude dynamic of the target can be written as

$$\dot{\boldsymbol{q}}_t = \frac{1}{2}\boldsymbol{q}_t \circ \begin{bmatrix} 0 \\ \boldsymbol{\omega}^t \end{bmatrix} \tag{1}$$

$$\boldsymbol{J}_t\dot{\boldsymbol{\omega}}^t + \boldsymbol{\omega}^t \times \left(\boldsymbol{J}_t\boldsymbol{\omega}^t\right) = \boldsymbol{0} \tag{2}$$

where $\circ$ is quaternion multiplication operator; $\boldsymbol{q}_t$ is attitude qaternion of the target, which represent rotation from $\mathcal{F}_I$ to $\mathcal{F}_t$; $\boldsymbol{\omega}^t = \boldsymbol{\omega}_a^t + \boldsymbol{\omega}_o^t$ is absolute angular velocity of the target, in which $\boldsymbol{\omega}_a^t$ is attitude angular velocity and $\boldsymbol{\omega}_o^t$ is orbit angular velocity; $\boldsymbol{J}_t$ is the the inertial matrix of the target ;

Similarly, the attitude dynamic of the servicer can be written as

$$\dot{\boldsymbol{q}}_s = \frac{1}{2}\boldsymbol{q}_s \circ \begin{bmatrix} 0 \\ \boldsymbol{\omega}^s \end{bmatrix} \tag{3}$$

$$\boldsymbol{J}_s\dot{\boldsymbol{\omega}}^s + \boldsymbol{\omega}^s \times \left(\boldsymbol{J}_s\boldsymbol{\omega}^s\right) = \boldsymbol{\tau}_t + \boldsymbol{\delta}_a \tag{4}$$

where $\boldsymbol{\tau}_t$ is the external torque applied to the servicer ; $\boldsymbol{\delta}_a$ is the disturbance torque ; Other symbols can refer to the target's.

The relative quaternion between the target and the servicer, in other word, the rotation from $\mathcal{F}_t$ to $\mathcal{F}_s$, can be defined as

$$\boldsymbol{q} = \boldsymbol{q}_t^{-1} \circ \boldsymbol{q}_s \tag{5}$$

Quaternion can be divided into scalar part and vector part. Therefore, the relative quaternion can also be written as,

$$\boldsymbol{q} = q_0 + \boldsymbol{q}_v \tag{6}$$

The relative angular velocity is defined as,

$$\boldsymbol{\omega} = \boldsymbol{\omega}^s - \boldsymbol{T}_{st}\boldsymbol{\omega}^t \tag{7}$$

in which $\boldsymbol{T}_{st}$ is the transition matrix form $\mathcal{F}_t$ to $\mathcal{F}_s$. It can be required by the relative quaternion $\boldsymbol{q}$ as following :

DOI: 10.13009/EUCASS2019-908

$$\boldsymbol{T}_{st} = \left(q_0^2 - q_v^T \boldsymbol{q}_v\right) I + 2q_v \boldsymbol{q}_v^T - 2q_0 \boldsymbol{q}_v^{\times} \tag{8}$$

The relative attitude dynamic based on relative quaternion can be formulized as

$$\dot{\boldsymbol{q}} = \frac{1}{2}\boldsymbol{q} \circ \begin{bmatrix} 0 \\ \boldsymbol{\omega} \end{bmatrix} \tag{9}$$

$$\dot{\boldsymbol{\omega}} = \dot{\boldsymbol{\omega}}^s - \dot{\boldsymbol{T}}_{st}\boldsymbol{\omega}^t - \boldsymbol{T}_{st}\dot{\boldsymbol{\omega}}^t \tag{10}$$

2.3 Relative Orbit Dynamic

The relative orbit dynamic equation between the target and the servicer in elliptical orbit[19] can be formulated as follows,

$$\ddot{\boldsymbol{x}}_L + \boldsymbol{A}_1\dot{\boldsymbol{x}}_L + \boldsymbol{A}_0\boldsymbol{x}_L = \boldsymbol{u} + \boldsymbol{\delta}_o \tag{11}$$

$$\boldsymbol{A}_1 = \begin{bmatrix} 0 & -2\omega_o^t & 0 \\ 2\omega_o^t & 0 & 0 \\ 0 & 0 & 0 \end{bmatrix} \tag{12}$$

$$\boldsymbol{A}_0 = \begin{bmatrix} -\left(\omega_o^t\right)^2 - \dfrac{2\mu}{r_T^3} & -\dot{\omega}_o^t & 0 \\ \ddot{\theta} & -\left(\omega_o^t\right)^2 + \dfrac{\mu}{r_T^3} & 0 \\ 0 & 0 & \dfrac{\mu}{r_T^3} \end{bmatrix} \tag{13}$$

where r_T is the distance from O_I to O_t; $\boldsymbol{x}_L = (x \;\; y \;\; z)^T$ is the relative position vector in $\mathcal{F}_L$, in which $\rho = \|\boldsymbol{x}_L\|$ is very small to r_T and satisfied $\rho / r_T \ll 1$; $\boldsymbol{u}$ is the control force of the servicer in frame $\mathcal{F}_L$; μ is the geocentric gravitational constant .

$\boldsymbol{u}$ is the projection of $\boldsymbol{u}_t$ in frame $\mathcal{F}_L$, and $\boldsymbol{u}_t$ is the control force of the servicer in frame $\mathcal{F}_t$. In addition, the desired position $\boldsymbol{x}_d$ of the service spacecraft is also in the target body coordinate frame and rotates with the target attitude. These result in the relative orbital motion coupled with the relative attitude parameters, which greatly increases the difficulty of path planning scheme constructing in next sections.

2.4 Safety workspace

In the scope of this paper, we address the autonomous on-orbit proximity manevour of planning a service spacecraft to approach a uncooperative target. To ensure the safety of this procedure, collision avoidance and restricted approaching direction (i.e. docking axis) must be guaranteed.

we suppose that the target is an ordinary satelliate with two solar panels on both sides along axis O_tY_t . A ellipsoid envelope is designed to prevent the servicer from crashing with attachments of the target. Semi-axises of the ellipsoid are ℓ, R, R respectively. Furthermore, in extra-close range (50~5 m), a circular conical surface along docking axis is proposed to ensure the trajectory of the servicer to progress inside.

It is noticed that traditional forbidden zone is designed as a static sphere, and the approaching corridor is along the V-bar or R-bar because the target is cooperative and attitude stabilization. In contrast, ellipsoid envelope and conical surface in this paper are fixed with the target and rotate in sapce. It keeps the safety workspace of the servicer more active and unconservative.

DOI: 10.13009/EUCASS2019-908

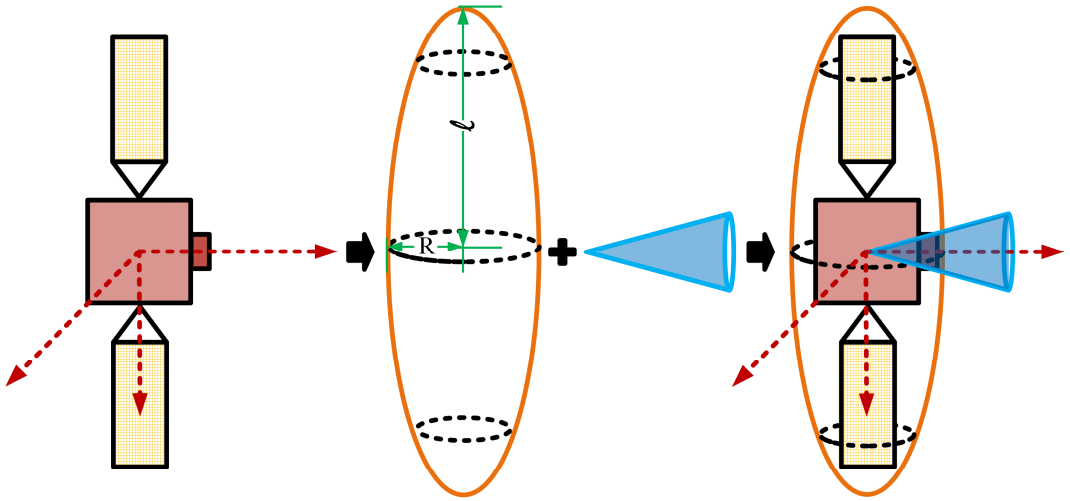

Figuer2 : Safety workspace

3. Artificial Potential Function

During the proximity mannuevor of driving the sevicer to approach the target, one crucial challenge is the threat of collision with components or even the main body of the target because the relative distance is extremely close. Once a deviation or a failure of the control system occour, the entire mission would turn into a disaster. While the Artificial Potential Function method can be applied to achieve safe proximity to avoid collisions.

The concept and essence of the Artificial Potential Function is to design a scalar function, which is a superposition of the attractive potential function and a series of repulsive potential functions. The attractive potential function is the global minimum set precisely in the desired location area, just like the valley bottom; the repulsive potential functions are set in the the forbidden area and the path constrained workspace respectively, just like multiple peaks. With proper control law designed, the service spacecraft will slide like a small ball to the valley and keep away from mounts.

3.1 Attractive Potential Function

In this paper, the attractive potential has no exception to formulate as a quadratic function as follows,

$$\varphi_a = \frac{1}{2}\left(\boldsymbol{x}_L - \boldsymbol{\chi}_d\right)^T \boldsymbol{P}_a \left(\boldsymbol{x}_L - \boldsymbol{\chi}_d\right) \tag{14}$$

where $\boldsymbol{P}_a$ is a symmetric, positive definite shaping matrix ; $\boldsymbol{\chi}_d$ is the desired terminal position in frame $\mathcal{F}_L$, which is $\boldsymbol{x}_d$ denoted in frame $\mathcal{F}_t$. The relation between $\boldsymbol{\chi}_d$ and $\boldsymbol{x}_d$ can be written as follow,

$$\boldsymbol{\chi}_d = \boldsymbol{T}_{Lt}\boldsymbol{x}_d \tag{15}$$

in which $\boldsymbol{T}_{Lt}$ is the transition matrix form $\mathcal{F}_L$ to $\mathcal{F}_t$.

3.2 Repulsive Potential Function

Referring to the analysis of safety worksapce in previous section, the repulsive potential functions are divided into two parts: 1) The servicer should be subject to forbidden zone around the target, i.e. the ellipsoid envelope. 2) The safety approach corridor.

The former part guarantees that the servicer maneuver to the target without collision during approaching process. The latter confine the trajectory to propagate in the absolute security field which varies with the attitude of the target.

DOI: 10.13009/EUCASS2019-908

3.2.1 Forbidden Zone

The forbidden zone of the target in this paper is an ellipsoid envelope depended on the target's geometry. The envelope is designed in frame $\mathcal{F}_t$, therefore it rolls with the target in space from $\mathcal{F}_I$ view. It can be expressed in frame $\mathcal{F}_t$ as an Guassian function,

$$\varphi_f = \psi_f \exp\left(-\frac{1}{2(\sigma_f)^2}|f_{env}|\right) \tag{16}$$

$$\begin{aligned} f_{env} &= \frac{x_t^2}{R^2} + \frac{y_t^2}{\ell^2} + \frac{z_t^2}{R^2} - 1 \\ &= \boldsymbol{x}_t^T \begin{bmatrix} R^2 & 0 & 0 \\ 0 & \ell^2 & 0 \\ 0 & 0 & R^2 \end{bmatrix} \boldsymbol{x}_t - 1 \end{aligned} \tag{17}$$

in which ψ_f and σ_f are the height and width parameters of Guassian function, respectively ; f_{env} is deformation of ellipsoid envelope equation.

3.2.2 Safety approaching Corridor

The safety approaching corridor is a circular conical surface, whose apex is at the target centroid, pointing to the axis OX_t , confined within $2 \bullet R$ long. The circular conical surface rotate with the docking axis which can be similarly expressed in frame $\mathcal{F}_t$ as an Guassian function,

$$\varphi_c = \psi_c \exp\left(-\frac{1}{2(\sigma_c)^2}|f_c|\right) \tag{18}$$

$$\begin{aligned} f_c &= \tan^2(\theta/2) x_t^2 - y_t^2 - z_t^2 \\ &= \boldsymbol{x}_t^T \begin{bmatrix} \tan^2(\theta/2) & 0 & 0 \\ 0 & -1 & 0 \\ 0 & 0 & -1 \end{bmatrix} \boldsymbol{x}_t \end{aligned} \tag{19}$$

in which $x_t \in [0, 2R]$; f_c is deformation of circular conical surface equation.

In order to make the potential function converge precisely to zero at the desired terminal position $\boldsymbol{x}_d$, the repulsive potential functions need some corections. After some manipulations, they are re-written as,

$$\varphi_f = \frac{1}{2}(\boldsymbol{x}_L - \boldsymbol{\chi}_d)^T \boldsymbol{P}_a (\boldsymbol{x}_L - \boldsymbol{\chi}_d) \bullet \psi_f \exp\left(-\frac{1}{2(\sigma_f)^2}|f_{env}|\right) \tag{20}$$

$$\varphi_c = \frac{1}{2}(\boldsymbol{x}_L - \boldsymbol{\chi}_d)^T \boldsymbol{P}_a (\boldsymbol{x}_L - \boldsymbol{\chi}_d) \bullet \psi_c \exp\left(-\frac{1}{2(\sigma_c)^2}|f_c|\right) \tag{21}$$

From the above, the whole artifitial potential function in this paper is deceloped as follow,

$$\varphi = \varphi_a + \varphi_f + \varphi_c \tag{22}$$

The contour of the potential function from $X_t Y_t$ plane can be obtained as figure 3.

DOI: 10.13009/EUCASS2019-908

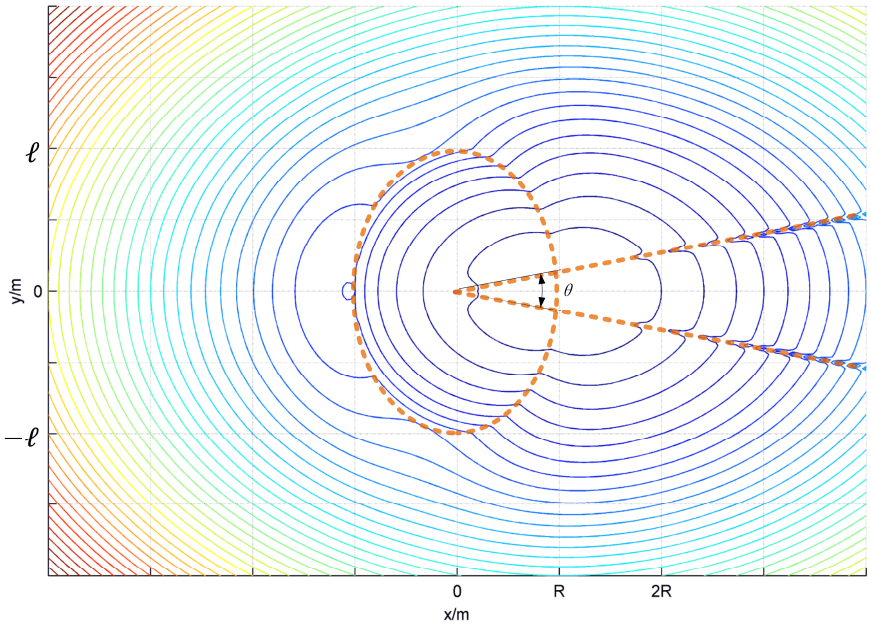

Figure 3 : Contour of whole potential field

4. Motion Planning of proximity maneuver

4.1 Uncooperative target attitude tracking

In analysis of relative motion equation, the raltive orbit is coupling with the relative attitude, while the opposite is not. A PD-like control law is designed to perform attitude synchronization between the servicer and the target. In other word, the relative attittude quaternion $\boldsymbol{q}$ should converge to$[1\ 0\ 0\ 0]^T$. Besides, the attitude quaternion (including the relative attitude quaternion) satisfy normalization constrain which means that we only need the vector part $\boldsymbol{q}_v$ converge to $\boldsymbol{0}$.

The relative attitude quaternion error is defined as,

$$\boldsymbol{e}_a = \boldsymbol{q}_v - \boldsymbol{0} = \boldsymbol{q}_v \tag{23}$$

After a few manipulation, we can obtain

$$\dot{\boldsymbol{e}}_a = \dot{\boldsymbol{q}}_v \tag{24}$$

$$\ddot{\boldsymbol{e}}_a = \ddot{\boldsymbol{q}}_v = -\frac{1}{4}(\boldsymbol{\omega}^T\boldsymbol{\omega})\boldsymbol{q}_v + \frac{1}{2}\boldsymbol{Q}^T f(\dot{\boldsymbol{\omega}}) + \frac{1}{2}\boldsymbol{Q}^T\boldsymbol{J}_s^{-1}(\boldsymbol{\tau}_t + \boldsymbol{\delta}_a) \tag{25}$$

where

$$\boldsymbol{Q} = q_0\boldsymbol{I}_3 + \boldsymbol{q}_v^{\times} \tag{26}$$

$$f(\dot{\boldsymbol{\omega}}) = -\boldsymbol{J}_s^{-1}\left\{(\boldsymbol{\omega}+\boldsymbol{T}_{st}\boldsymbol{\omega}_t)\times[\boldsymbol{J}_s(\boldsymbol{\omega}+\boldsymbol{T}_{st}\boldsymbol{\omega}_t)]\right\} + \boldsymbol{T}_{st}\boldsymbol{J}_s^{-1}[\boldsymbol{\omega}_t\times(\boldsymbol{J}_t\boldsymbol{\omega}_t)] + \boldsymbol{\omega}\times(\boldsymbol{T}_{st}\boldsymbol{\omega}_t) \tag{27}$$

Define a matrix $\boldsymbol{A}$ as follow,

$$\boldsymbol{A} = \frac{1}{2}\boldsymbol{Q}^T\boldsymbol{J}_s^{-1} \tag{28}$$

and a PD-like control law is designed,

$$\boldsymbol{\tau}_t = -\boldsymbol{A}^{-1}[\boldsymbol{K}_p\boldsymbol{e}_q + \boldsymbol{K}_D\dot{\boldsymbol{e}}_q - \frac{1}{4}(\boldsymbol{\omega}^T\boldsymbol{\omega})\boldsymbol{q}_v + \frac{1}{2}\boldsymbol{Q}^T f(\dot{\boldsymbol{\omega}})] \tag{29}$$

DOI: 10.13009/EUCASS2019-908

where the $\boldsymbol{K}_P$ and $\boldsymbol{K}_D$ are positive diagonal control parameter matrixes.

4.2 Path planning of proximity maneuver

For safety concern, both forbbiden zone and approaching corridor should be incorporated into path planning of the servicer.Define a sliding mode surface according to the Sliding Mode Control(SMC) theory,

$$\boldsymbol{e}_o = \boldsymbol{x}_L - \boldsymbol{\chi}_d \tag{30}$$

$$\boldsymbol{s} = k\nabla_{\boldsymbol{x}_L}\varphi + \dot{\boldsymbol{e}}_o \tag{31}$$

The time derivation of equation (31) can be acquired,

$$\dot{\boldsymbol{s}} = k\frac{d}{dt}\nabla_{\boldsymbol{x}_L}\varphi + \ddot{\boldsymbol{e}}_o \tag{32}$$

A sliding mode reach law is defined as,

$$\dot{\boldsymbol{s}} = -\boldsymbol{\lambda}_1\boldsymbol{s} - \boldsymbol{\lambda}_2\,\mathrm{sgn}(\boldsymbol{s}) \tag{33}$$

in which $\boldsymbol{\lambda}_1$ and $\boldsymbol{\lambda}_2$ are positive definite matrixes.

Incorporating equation (11), a safety control law based on APF can be formulated as,

$$\boldsymbol{u}_t = -\lambda_1\boldsymbol{s} - \lambda_2\,\mathrm{sgn}(\boldsymbol{s}) - k\frac{d}{dt}\nabla_{\boldsymbol{\rho}_L}\varphi + \ddot{\boldsymbol{\chi}}_d + \boldsymbol{A}_1\dot{\boldsymbol{x}}_L + \boldsymbol{A}_0\boldsymbol{x}_L \tag{34}$$

where

$$\nabla_{\boldsymbol{x}_L}\varphi = \nabla_{\boldsymbol{x}_L}\varphi_a + \nabla_{\boldsymbol{x}_L}\varphi_f + \nabla_{\boldsymbol{x}_L}\varphi_c \tag{35}$$

$$\begin{cases} \nabla_{\boldsymbol{x}_L}\varphi_a = \boldsymbol{P}_a\left(\boldsymbol{x}_L - \boldsymbol{\chi}_d\right) \\ \nabla_{\boldsymbol{x}_L}\varphi_f = \varphi_f^E \bullet \nabla_{\boldsymbol{x}_L}\varphi_a + \varphi_a \bullet \nabla_{\boldsymbol{x}_L}\varphi_f^E \\ \nabla_{\boldsymbol{x}_L}\varphi_c = \varphi_c^E \bullet \nabla_{\boldsymbol{x}_L}\varphi_a + \varphi_a \bullet \nabla_{\boldsymbol{x}_L}\varphi_c^E \end{cases} \tag{36}$$

$$\begin{cases} \nabla_{\boldsymbol{x}_L}\varphi_f^E = \psi_f \exp\left(-\dfrac{1}{\sigma_f}\left|f_{env}\right|\right) \bullet \left(-\dfrac{1}{\sigma_f}\dfrac{\partial\left|f_{env}\right|}{\partial\boldsymbol{x}_L}\right) \\ \nabla_{\boldsymbol{x}_L}\varphi_c^E = \psi_c \exp\left(-\dfrac{1}{\sigma_c}\left|f_c\right|\right) \bullet \left(-\dfrac{1}{\sigma_c}\dfrac{\partial\left|f_c\right|}{\partial\boldsymbol{x}_L}\right) \end{cases} \tag{37}$$

5. Simulation Results

In this section, a series of numerical simulations are presented to demonstrate the performance of the motion planning method proposed in this paper. Firstly, the servicer tracks precisely the attitude of uncooperative tumbling target on elliptical orbit with small eccentricities. Then, the trajectory of servicer will be designed to get close to the uncooperative target with attitude synchronization, avoiding the main-body and components to ensure the safety during the process. Eventually, the servicer reach the desired terminal position after getting through the approaching corridor. In contrast, PD-like control would also be applied for trajectory planning to reveal the advantage of APF in this paper.

Simulation parameters relevant to the target and the servicer are listed in Table 1. $[i,\Omega,\omega,\theta_0]$ are inclination, RAAN, argument of perigee, and true anomaly, respectively.

Table 1: Simulation parameters

Parameter	Value	Unit
Semi-major axis, a	7178.160	km
Eccentriccity, e	0.005	-
Other orbital parameters, $[i,\Omega,\omega,\theta_0]$	[60,45,30,0]	(°)

DOI: 10.13009/EUCASS2019-908

Inertial moment of the target, $\boldsymbol{J}_t$	diag(160,150,200)	$kg{\cdot}m^2$
Inertial moment of the servicer, $\boldsymbol{J}_s$	diag(150,190,240)	$kg{\cdot}m^2$
Initial attitude quaternion of the target, $\boldsymbol{q}_t$	$[0.8\ 0.2\ -0.4\ 0.4]^T$	-
Initial attitude quaternion of the servicer, $\boldsymbol{q}_s$	$[\sqrt{2}/2\ \ 0.5\ 0.3\ -0.4]^T$	-
Initial attitude angular velocity of the target, $\boldsymbol{\omega}_a^t$	$[-3\ 2\ 3]^T$	$°/s$
Initial attitude angular velocity of the servicer, $\boldsymbol{\omega}_a^s$	$[-0.02\ 0.01\ 0.02]^T$	$°/s$
Initial relative position, $\boldsymbol{r}_{L0}$	$[45\sqrt{2}\ -25\ 70]^T$	m
Initial relative velocity, $\dot{\boldsymbol{r}}_{L0}$	$[-0.25\ 0.1\ -0.3]^T$	m/s
Semi-major axis of ellipsoid, ℓ	10	m
Semi-middle and Semi-minor axis of ellipsoid, R	5	m

5.1 Attitude synchronization

In this simulation, $\boldsymbol{K}_P$ and $\boldsymbol{K}_D$ are set as $diag([0.14\ \ 0.14\ \ 0.14])$ and $diag([0.8\ \ 0.8\ \ 0.8])$ based on equations in section 4.1. The process of tracking the attitude of the target is illustrated in figure 4, which shows the changes between two body coordinate frame $\mathcal{F}_t$ and $\mathcal{F}_s$ in 200 seconds.

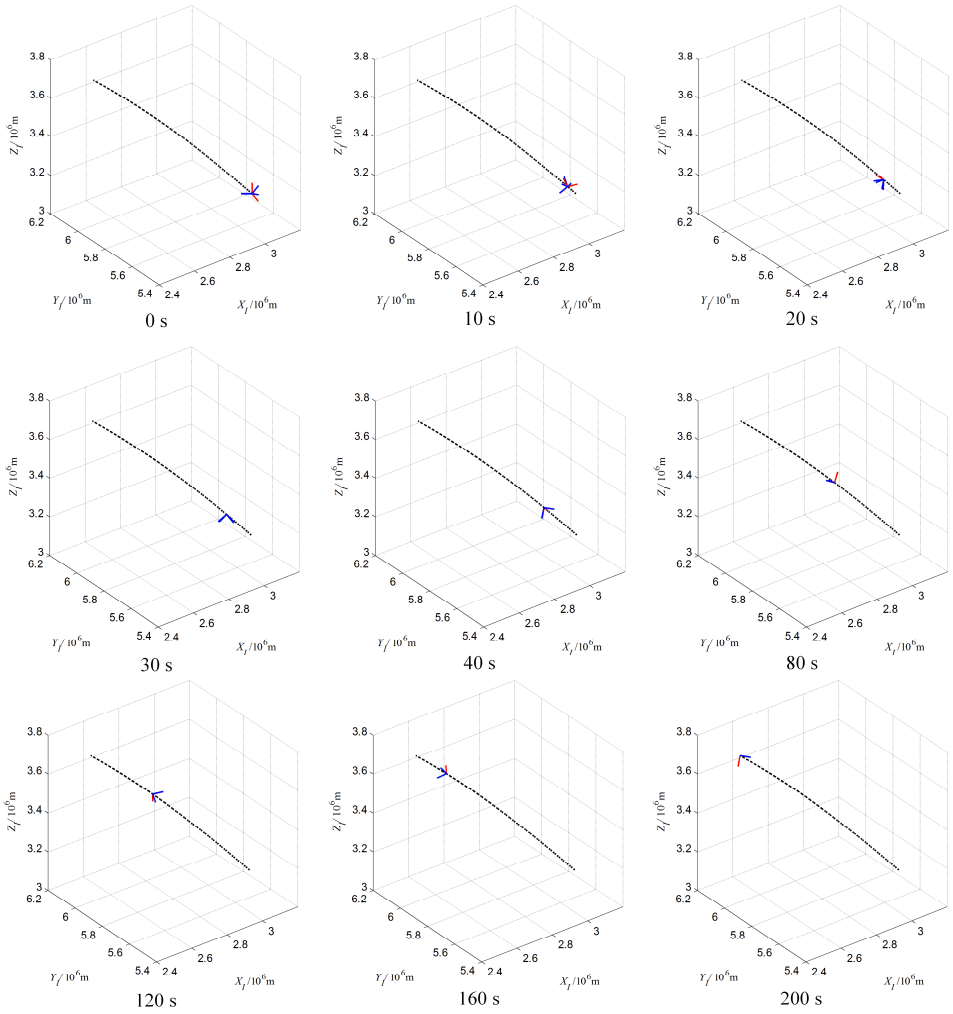

Figure 4 : Attitude tracking in frame $\mathcal{F}_I$

Figure 5 shows the time response of the relative quaternion. It can be found that $\boldsymbol{q}$ converge to $[1\ 0\ 0\ 0]^T$ at about 40s which imply that the servicer's attitude is synchronizing with the tumbling target.

DOI: 10.13009/EUCASS2019-908

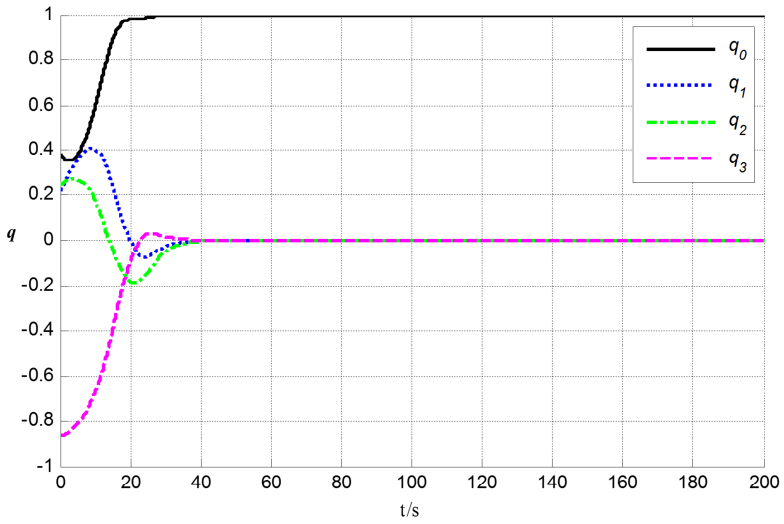

Figure 5 : Time response of the relative attitude queternion $\boldsymbol{q}$

5.2 Path planning

5.2.1 Path planning based on PD-like controller

In previous simulation, the servicer achieve attitude tracking with the target independently within 200s. However, the relative orbital motion is coupled with the relative attitude which can be found in analysis of section 2. Based on the calculation or measurement data of the relative attitude, a PD-like control law is designed to achieve the approximation of the target. In this simulation, $\boldsymbol{K}_P$ and $\boldsymbol{K}_D$ are set as $diag$[0.38 0.38 0.38] and $diag$[1.4 1.4 1.4], respectively. Figure 6 gives the trajectory of the servicer in $\mathcal{F}_t$. In Figure 7, the trajectory in 2D demonstrates the location relationship among the service spacecraft, the forbidden zone and the approaching corridor, and then the simulation results with the initial relative position changes are utilized as comparison. The trajectory departing from the start1 cross the conical surface, the trajectory from start2 ($\boldsymbol{r}_{L0} = [-45\sqrt{2}\ 25\ -70]^T$) violate both the forbidden zone constraint and the safety corridor constraint which could lead to collision and failure. The result imply that a pure PD-like controller cannot guarantee the safety of the trajectory and the accuracy of the approaching direction.

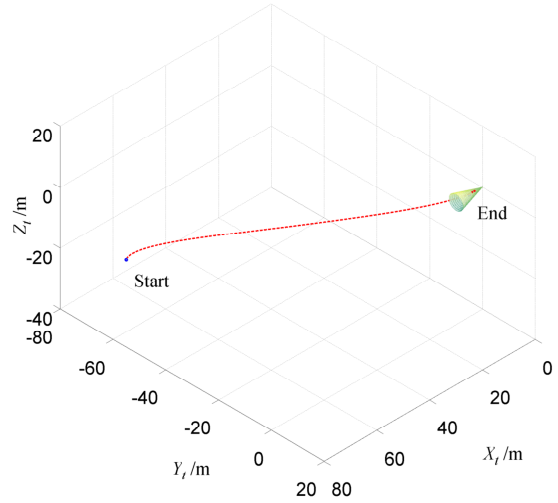

Figure 6 : The trajectory of the servicer in $\mathcal{F}_t$ based on PD-like control

DOI: 10.13009/EUCASS2019-908

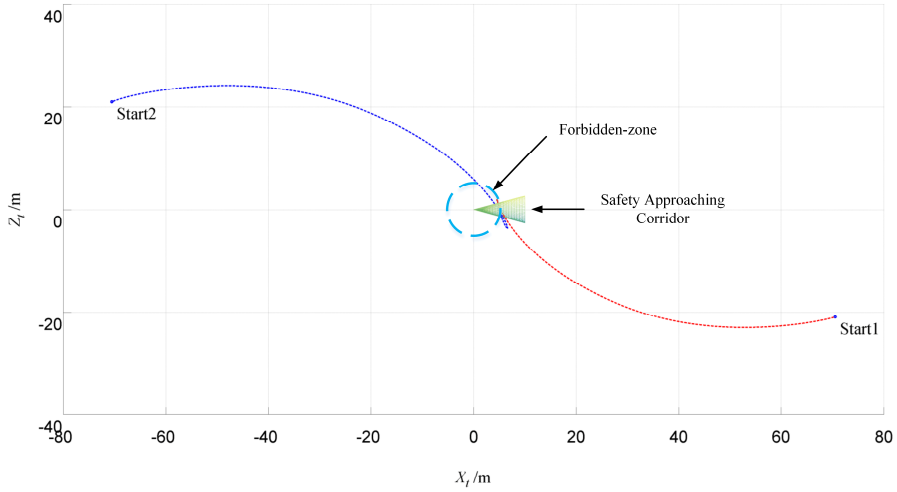

Figure 7 : Trajectory from different initial position in X_tY_t plane

5.2.2 Path planning based on APF method

The purpose of the servicer is collision avoidance and reaching the desired position in limited approaching direction with attitude synchronization. Therefore, a APF-based path planning method is given in section 4.2. In this simulation, the shaping matrix $\boldsymbol{P}_a$ is set as $\boldsymbol{I}_{3\times3}$, ;Height and width parameter of Guassion functions lke $[\psi_f \ \sigma_f \ \psi_c \ \sigma_c]$ are set as $[0.5 \ 1.5 \ 0.8 \ 1.2]$; λ_1 and λ_2 are set as 0.15 and 0.1 respectively.

Figure 8 shows the time response of the relative position under APF-based path planning method proposed in this paper. In frame $\mathcal{F}_t$, $\boldsymbol{x}_t$ converge to the desired terminal position $[5\ 0\ 0]^T$. Considering the relative attitude quaternion response in last section, figure 9 illustrates the orbit and attitude time-varying relationship between the servicer and the target in frame $\mathcal{F}_L$. For descriped clearly, the scope of the safety corridor has been reduced. In addition, it should be noted that in this simulation, the forbidden zone and the approaching corridor are not static but rotated with the target attitude.

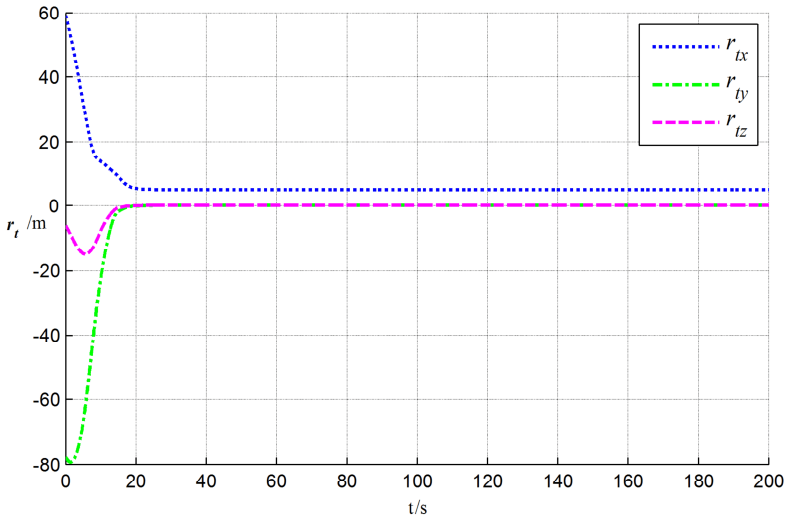

Figure 8 : Time response of the relative position in frame $\mathcal{F}_t$

Figure 10 shows a 3-dimensional view of the trajectory in freame $\mathcal{F}_t$. After changing the initial relative position, the trajectory changes as shown in Figure 11. The projection comparison in plane X_tZ_t of the 3-dimensional trajectory from two starting points is given in Figure 12.

DOI: 10.13009/EUCASS2019-908

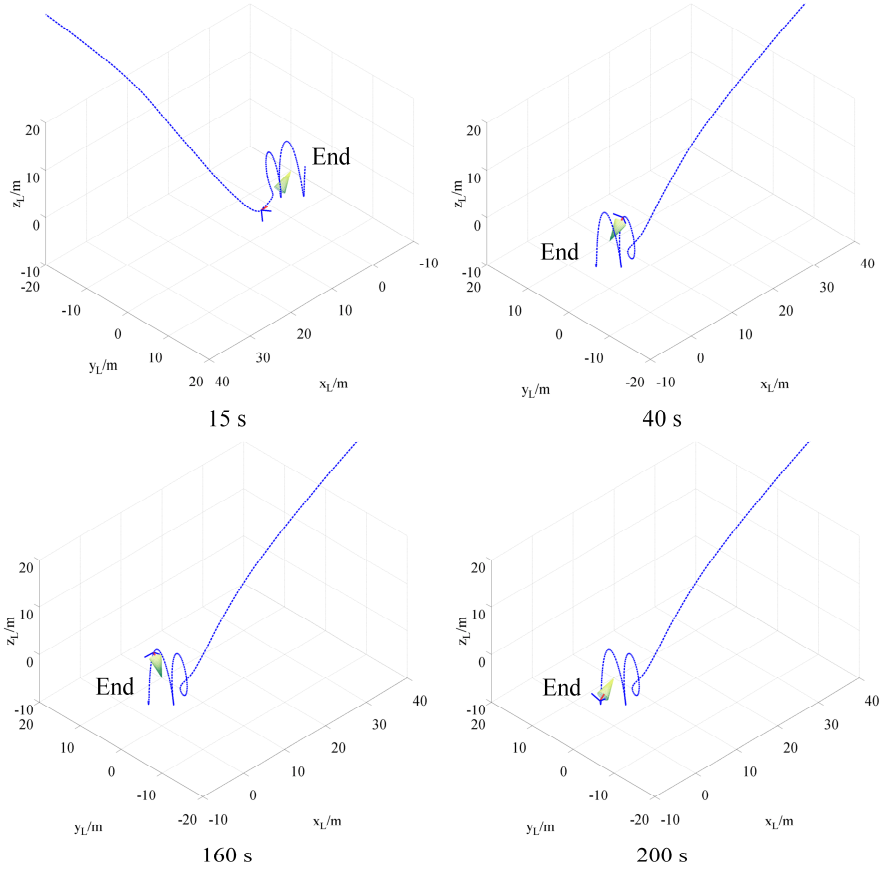

Figure 9 : Collaborative planning of the orbit and attitude in frame $\mathcal{F}_L$

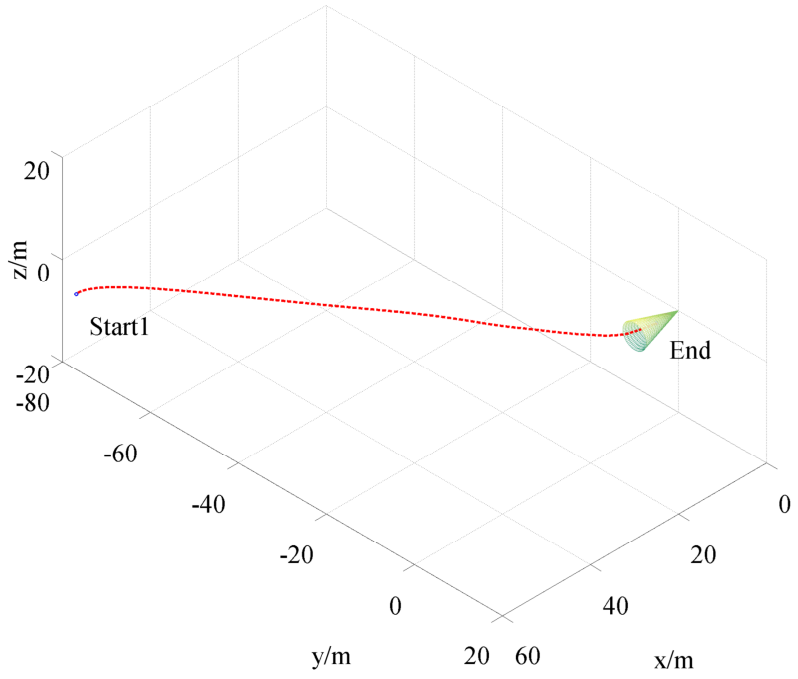

Figure 10 : 3D view of the trajectory in freame $\mathcal{F}_t$ from start1

DOI: 10.13009/EUCASS2019-908

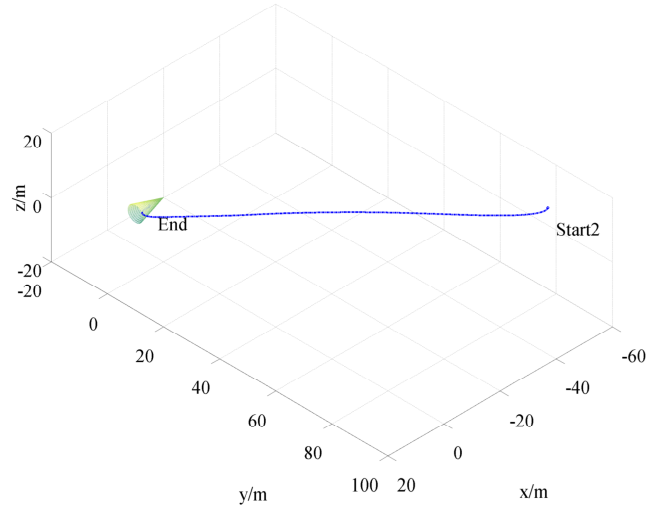

Figure 11 : 3D view of the trajectory in freame $\mathcal{F}_t$ from start2

Comparing with the results of the previous section, the path planning based on APF method, combined with the attitude synchronization, will realize that the servicer actively evades the target spacecraft body and components and arrive at the desired position from the approaching corridor. It is successfully applied to any initial state and even the target is uncooperative.

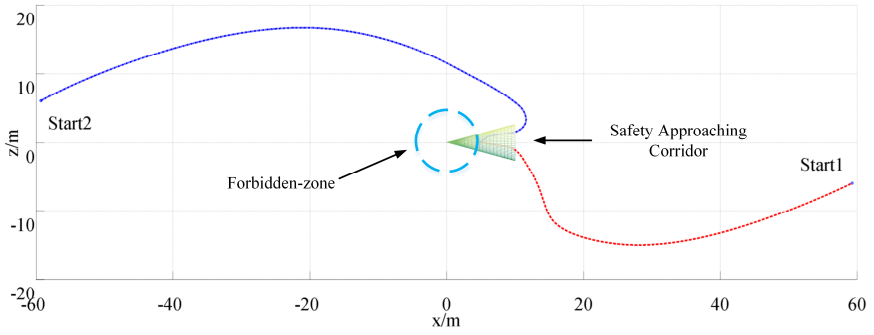

Figure 12 : Trajectory projection comparison in plane X_tZ_t from two different starting points

6.Conclusion

In this paper, the attitude-orbit coupling model of spacecraft relative motion is established. The independence of relative attitude motion and the relative orbit motion coupling with attitude are analyzed. Coupling factors include control force of the servicer and the desired position related to the target. An ellipsoidal forbidden zone and a conical surface approaching corridor are designed to guarantee motion safety and restricted access. An unique potential function considering both safety workspace and final state are formulated based on APF method, and sliding mode control is introduced in numerical simulations. Results show that approaching trajectories of the servicer satisfy the safety workspace and desired state from any initial position. It is compared with a PD-like controller and the availability of this method in this paper is proved.

References

[1] Davis T M , Melanson D . XSS-10 microsatellite flight demonstration program results[J]. Proceedings of SPIE - The International Society for Optical Engineering, 2004, 5419.

[2] Rumford T E . Demonstration of autonomous rendezvous technology (DART) project summary[C]// Space Systems Technology & Operations. Space Systems Technology and Operations, 2003.

DOI: 10.13009/EUCASS2019-908

[3] Shoemaker J , Wright M . Orbital express space operations architecture program[J]. Proceedings of SPIE - The International Society for Optical Engineering, 2004, 5088:1-9.
[4] Barnhart D, Sullivan B, Hunter R, et al. Phoenix program status-2013[C]//AIAA SPACE 2013 conference and exposition. 2013: 5341.
[5] Nolet S , Kong E , Miller D W . Autonomous docking algorithm development and experimentation using the SPHERES testbed[J]. Proceedings of SPIE - The International Society for Optical Engineering, 2004, 5419(5419).
[6] Oda M. ETS-VII: achievements, troubles and future[C]//Proceedings of the 6th International Symposium on Artificial Intelligence and Robotics & Automation in Space: ISAIRAS 2001. 2001.
[7] Lizarralde F , Wen J T . Attitude control without angular velocity measurement: a passivity approach[C]// Proceedings of 1995 IEEE International Conference on Robotics and Automation. IEEE, 2002.
[8] Jin E , Sun Z . Robust controllers design with finite time convergence for rigid spacecraft attitude tracking control[J]. Aerospace Science and Technology, 2008, 12(4):324-330.
[9] Zou A M , Kumar K D . Quaternion-Based Distributed Output Feedback Attitude Coordination Control for Spacecraft Formation Flying[J]. Journal of Guidance, Control, and Dynamics, 2013, 36(2):548-556.
[10] Yang, Yaguang. An efficient algorithm for periodic Riccati equation with periodically time-varying input matrix[J]. Automatica, 2017, 78:103-109.
[11] Roger A B , Mcinnes C R . Safety Constrained Free-Flyer Path Planning at the International Space Station[J]. Journal of Guidance, Control, and Dynamics, 2000, 23(6):971-979.
[12] Lu P , Liu X . Autonomous Trajectory Planning for Rendezvous and Proximity Operations by Conic Optimization[J]. Journal of Guidance, Control, and Dynamics, 2013, 36(2):375-389.
[13] Liu X , Lu P . Solving Nonconvex Optimal Control Problems by Convex Optimization[J]. Journal of Guidance, Control, and Dynamics, 2014, 37(3):750-765.
[14] Breger L S , How J P . Safe Trajectories for Autonomous Rendezvous of Spacecraft[J]. Journal of Guidance, Control, and Dynamics, 2008, 31(5):1478-1489.
[15] Khatib O . Real-Time Obstacle Avoidance System for Manipulators and Mobile Robots[J]. International Journal of Robotics Research, 1986, 5(1):90-98.
[16] Martinson N , Munoz J D . A new method of guidance control for autonomous rendezvous in a cluttered space environment[C]// Collection of Technical Papers - AIAA Guidance, Navigation, and Control Conference 2007, 2013.
[17] St. Johnolcayto E , Mcinnes C R , Ankersen F . Safety-critical autonomous spacecraft proximity operations via potential function guidance[C]// Aiaa Infotech. 2007.
[18] Munoz J D . Rapid path-planning algorithms for autonomous proximity operations of satellites[J]. Dissertations & Theses - Gradworks, 2011.
[19] Melton, Robert G . Time-Explicit Representation of Relative Motion Between Elliptical Orbits[J]. Journal of Guidance, Control, and Dynamics, 2000, 23(4):604-610.